

Artigo de Pesquisa

Conditioning Factors in the Formation of the Inverted Intra-lagoon Delta of the Urussanga Velha Lagoon, Southern Santa Catarina, Brazil

Fatores Condicionantes na Formação do Delta Intralagunar Invertido da Lagoa Urussanga Velha, Sul de Santa Catarina, Brasil

Renato Amabile Leal¹ , Eduardo Guimarães Barboza^{1,2} , Mauro Michelena Andrade³  & Volney Júnior Borges Bitencourt⁴ 

¹UFRGS, Programa de Pós-Graduação em Geociências, Porto Alegre, Brasil. relealsc@gmail.com.

²UFRGS, Centro de Estudos de Geologia Costeira e Oceânica, Porto Alegre, Brasil. eduardo.barboza@ufrgs.br.

³UNIVALI, Programa de Pós-Graduação em Ciência e Tecnologia Ambiental, Itajaí, Brasil. michelena@univali.br.

⁴IMA, Instituto do Meio Ambiente de Santa Catarina, Florianópolis, Brasil. volneybitencourt@gmail.com.

Abstract: The Southern Santa Catarina Coastal Plain is formed by the overlapping of sedimentary deposits of two lagoon/barrier depositional systems. One of the lagoons of the most recent system (holocenic) presents an intra-lagoon delta of peculiar morphology. This delta is formed from the ocean into the lagoon. The present study aimed to identify which are the factors responsible for the formation and evolution of this morphological feature. To identify the conditioning factors involved, a spatiotemporal analysis was conducted between 1957 and 2012. Remote sensing data was used to identify hydrodynamic patterns. This data was analyzed together with water parameters (turbidity and salinity) and relative sea level. The correlation between this information and climatological data (low and very low-frequency climate variabilities) was also integrated. The main conditioning factors identified included: phase changes of the Pacific Decadal Oscillation (PDO) and of the El Niño - Southern Oscillation (ENSO); the influence of positive low-frequency sea-level oscillations (storm surge); and human interference. Both climate variability modes were associated with a high occurrence of rainfall in the region, which consequently provided a high availability of sediments in the Urussanga River fluvial-estuarine system. In addition to influencing rainfall increase, periods, when El Niño predominated, tended to result in a high occurrence of positive storm surges, which influenced the hydrodynamic flow responsible for transporting sediment towards the lagoon's interior and, consequently, for forming the delta.

Keywords: Climate Variability; ENSO; PDO; Hydrodynamics; Teleconnections.

Resumo: A Planície Costeira Sul Catarinense é formada pela sobreposição de depósitos sedimentares de dois sistemas deposicionais laguna/barreira. Uma das lagoas do sistema, mais recente (holocênico), apresenta um delta intralagunar de morfologia peculiar. Este delta é formado na direção do oceano para o continente. O presente estudo teve como objetivo identificar quais são os fatores responsáveis pela formação e evolução desta feição morfológica. Para identificar os fatores condicionantes envolvidos, foi realizada uma análise espaço-temporal entre 1957 e 2012. Dados de Sensoriamento Remoto foram utilizados para identificar os padrões hidrodinâmicos. Esses dados foram analisados em conjunto com parâmetros hídricos (turbidez e salinidade) e nível relativo do mar. A correlação entre esses parâmetros e os dados climatológicos (variabilidades climáticas de baixa e muito baixa frequência) também foram integrados. As principais condicionantes identificadas incluíram: mudanças de fase da Oscilação Decadal do Pacífico (PDO) e do El Niño - Oscilação Sul (ENSO); a influência das oscilações positivas do nível do mar de baixa frequência (ondas de tempestades); e a interferência humana. Ambos os modos de variabilidade climática estiveram associados à elevada ocorrência de chuvas na região, o que conseqüentemente, proporcionou alta disponibilidade de sedimentos no sistema flúvio-estuarino do rio Urussanga. Além de influenciar no aumento das chuvas, os períodos de predominância do El Niño tenderam a resultar em elevada ocorrência de tempestades positivas, o que influenciou o fluxo hidrodinâmico responsável pelo transporte de sedimentos para o interior da lagoa e, conseqüentemente, pela formação do delta.

Palavras-chave: Variabilidade Climática; ENSO; ODP; Hidrodinâmica; Teleconexões.

1. Introduction

Morphological changes in coastal zones vary throughout time and space and result from the interaction between dynamic processes and local morphology, supported by specific geological context (Cowell *et al.*, 2006; Kinsela *et al.*, 2020). These dynamic processes include waves, tides, currents, and winds. All of these provide the energy that shapes and changes the coast, by eroding, transporting, and depositing sediments along the shoreline over time. Deltas are coastal environments of high geological and geomorphological importance because they are a great source of coastal sediments. Fluvial deltas are mostly formed along the margins of marine basins, and the deltas of some major rivers are considered the largest coastal forms in the world (Evans, 2012). Modern deltas are widely variable regarding their scale, processes, and nature of the sediments deposited. Scales encompass several orders of magnitude, presenting radiuses ranging from less than 1 to more than 100 km, and evolution periods between a few years and several millions of years. The development and dimension of these features depend on a series of conditions, which include grain size and evolution characteristics of tectonic plates (Orton & Reading, 1993; Davis Jr. & FitzGerald, 2004; Anthony, 2014).

Definitions, classifications, formation factors, and other characteristics have been increasingly investigated in depth as a result of the progress of studies and the advances in technologies and methodologies used. However, these studies have focused on large-scale (spatiotemporal) features in fluvial-marine environments (Galloway, 1975; Coleman & Wright, 1975; Orton & Reading, 1993; Dalrymple, 1999), where allogenic conditioning factors (climate, tectonics, and marine eustatic level) predominate. Delta formation and evolution result from processes that occur in various spatiotemporal scales combining allogenic and autogenic processes (Jerolmack & Paola, 2010; Straub & Esposito, 2013; Karamitopoulos *et al.*, 2014; Rocha & Rosa, 2021).

Allogenic processes are those of global and regional dimensions, associated with external drivers to the sedimentary system, mainly characterized by changes in base level. On the other hand, autogenic processes present local dimension and are related to an exclusively sedimentary prism, from the systems' internal energy gradients, without large changes in hydrodynamics, sediment input, and/or slope of the receiving basin (Beerbower, 1966; Sutter, 1994). According to Rosa *et al.* (2016), allogenic controls are applicable at a basin scale, where they contribute to the understanding and translation of depositional environments in space and time. However, regarding smaller deltas, autogenic processes are predominant.

Recent studies explain that autogenic processes acting over long time scales control the regularity or instability in which basins are filled (Kim *et al.*, 2006; Straub *et al.*, 2009). Therefore, even in environments where allogenic sources are constant, small-scale processes can be influential. To what extent allogenic and autogenic processes contribute to the morphological evolution of fluvial-deltaic systems is still under debate (Kim *et al.*, 2006; Van Dijk *et al.*, 2009; Tomer *et al.*, 2011). According to Karamitopoulos *et al.* (2013), our knowledge of the roles of the various autogenic processes is at best insufficient, and whether these processes interact or are ultimately conducted by allogenic mechanisms is still unknown.

The emerged portion of the Pelotas Basin, Brazil, is of particular interest because it encompasses numerous Holocene lake and lagoon systems, formed during the evolution of Lagoon-Barrier Systems II, III, and IV (Villwock *et al.*, 1986). The form of Lagoon-Barrier System IV shows the formation of intra-lagoon deltas. Recently, Rocha & Rosa (2021) addressed the morphodynamic variability of these deltas found on the northern coast of the state of Rio Grande do Sul. They identified a particular type of delta and associated its formation with aeolian systems in sectors where the shoreline presents transgressive behavior.

The delta studied is located in the southern portion of the coastal plain of the state of Santa Catarina and is part of a complex fluvial-estuarine system of the Urussanga River. The Urussanga River springs from the slopes of the Eastern Serra Catarinense mountain range and crosses the coastal plain since the transitional Pleistocene deposits (Barrier III), cutting the Holocene barrier (Barrier IV) to the Atlantic Ocean (Leal *et al.*, 2021). Before flowing into the ocean, the river has a confluence that connects it to the Urussanga Velha Lagoon. This river-lagoon connection is responsible for forming an intra-lagoon delta of peculiar morphology, positioned in a relatively inverted way compared with the regular flow of commonly found intra-lagoon deltas. Due to this morphology, sediments that form this feature are believed to be transported across the estuary under specific climatological and oceanographic conditions. Thus, the objective of the present study was to understand the conditioning factors for the formation and evolution of the intra-lagoon delta of the Urussanga Velha Lagoon.

1.1 General characteristics of the study area

The study area is located at the border between the municipalities of Balneario Rincão and Jaguaruna (Southern Coast, Balneario Torneiro – Fig. 1). The region is within the northern portion of the Pelotas Basin, which corresponds to the Southern Santa Catarina Coastal Plain. According to Fernandez *et al.* (2019), this coastal plain is characterized by sandy coastal barriers and lagoons formed during the Quaternary. The barrier morphology is defined by the presence of transgressive sand sheets (TSS) and the stratigraphic stacking pattern is progradational, characterizing a regressive type of barrier (Leal *et al.*, 2016;

Barboza & Leal, 2017). It also presents a low slope, and its formation is associated with the glacio-eustatic sea-level changes that occurred during the Quaternary, which resulted in the overlapping of sedimentary deposits associated with lagoon/barrier depositional systems (Villwock *et al.*, 1986). According to Rosa *et al.* (2011, 2017), these depositional systems correspond to high-frequency depositional sequences.

The northern portion of the Pelotas Basin marks a change in the direction of the coastline in southern Brazil, with a mainly NE-SW orientation which is exposed to all wave and wind directions. Wave characteristics reflect the wind regime over the South Atlantic. Therefore, during the austral spring and summer, waves are predominantly from the eastern quadrant. In turn, during the austral autumn and winter, the passing of frontal systems produces winds and waves from the southern quadrant (Araújo *et al.*, 2003).

The coast of Santa Catarina presents a microtidal regime with semi-diurnal characteristics, ranging from 1.05 m in the north to 0.46 m in the south (Klein *et al.*, 2016). According to Siegle & Calliari (2008), during cold front meteorological events, strong winds from the southern quadrant with mean speed values of 8 ms^{-1} induce sea-level rise along the coast. Andrade *et al.* (2018) observed that a low-frequency sea-level oscillation (storm surge) reached 0.66 m above mean sea level in the northern coast of Rio Grande do Sul. Therefore, when large ranges of astronomical tides and storm surges are combined, extreme sea-level rise events can occur along the coast.

The longshore drift in the Pelotas Basin is controlled by waves from the southern quadrant that, although less frequent, are more intense. However, Siegle & Asp (2007) concluded that the longshore drift between the mouth of the Araranguá River and the Santa Marta Cape, over an annual period, is bidirectional, with a clear decrease in transport potential. However, Barboza *et al.* (2014), Biancini da Silva *et al.* (2014), and Becker *et al.* (2021) demonstrate a long-term resultant drift of the Araranguá, Mampituba, and Urussanga rivers to NE.

Sea-level curves close to the study area indicate that during the culminating point of the Post-glacial Marine Transgression (PMT) around 5 ka ago, the sea level was approximately 1-3 m above its current level; after that, it slowly began to fall (Barboza & Tomazelli, 2003; Barboza *et al.*, 2021; Angulo *et al.*, 2022). Records of specific relative sea-level positions during the Holocene obtained in studies along the coastal plain of Rio Grande do Sul and Santa Catarina states fit within the envelopes of these curves.

According to the Köppen climate classification, the region is classified as Cfa, humid subtropical, oceanic, without a dry season, and with warm summers (Alvares *et al.*, 2014). The interaction between the atmosphere and the ocean occurs through various processes. However, wind is the main force that affects surface ocean circulation. In the study area, the position of the South Atlantic Subtropical Anticyclone and its seasonal variability are factors that directly affect wind intensity and direction. During austral summers, wind is predominantly from the east-northeast between latitudes 15°S and 35°S . In turn, during austral winters, this same direction can only be observed between 20°S and 25°S , while south of 25°S the predominant wind direction is west-southeast (Taschetto, 2006). This wind direction pattern is modified by the passing of extratropical cyclones, which are low-pressure transitory mobile systems with clockwise circulation in the southern hemisphere. They occur more frequently during austral winters and are usually associated with frontal systems with strong air temperature gradients. During the passing of these cyclones, the intense winds produced are from the south-southwest (Brusius *et al.*, 2020).

In southern and southeastern Brazil, winds from the southern quadrant generate a resultant water transport from the open sea towards the coast, causing an accumulation of

water on the coast and, consequently, a low-frequency sea-level rise, usually called “storm surge” (Truccolo *et al.*, 2006). In other words, episodes where sea level is higher than average, in low frequencies, are a response to surface ocean currents towards the coast.

Large-scale climatic events and ocean-atmosphere interactions also influence southern Brazil, changing rainfall, wind, wave, and current patterns (Grimm *et al.*, 1998; Schossler *et al.*, 2018); the El Niño - Southern Oscillation (ENSO) is among the most investigated and known of these phenomena. In years when El Niño occurs, the southern region experiences an increase in rainfall during austral springs, with a pronounced peak during November, while during La Niña periods, intense and regular droughts occur (Schneider & Gies, 2004).

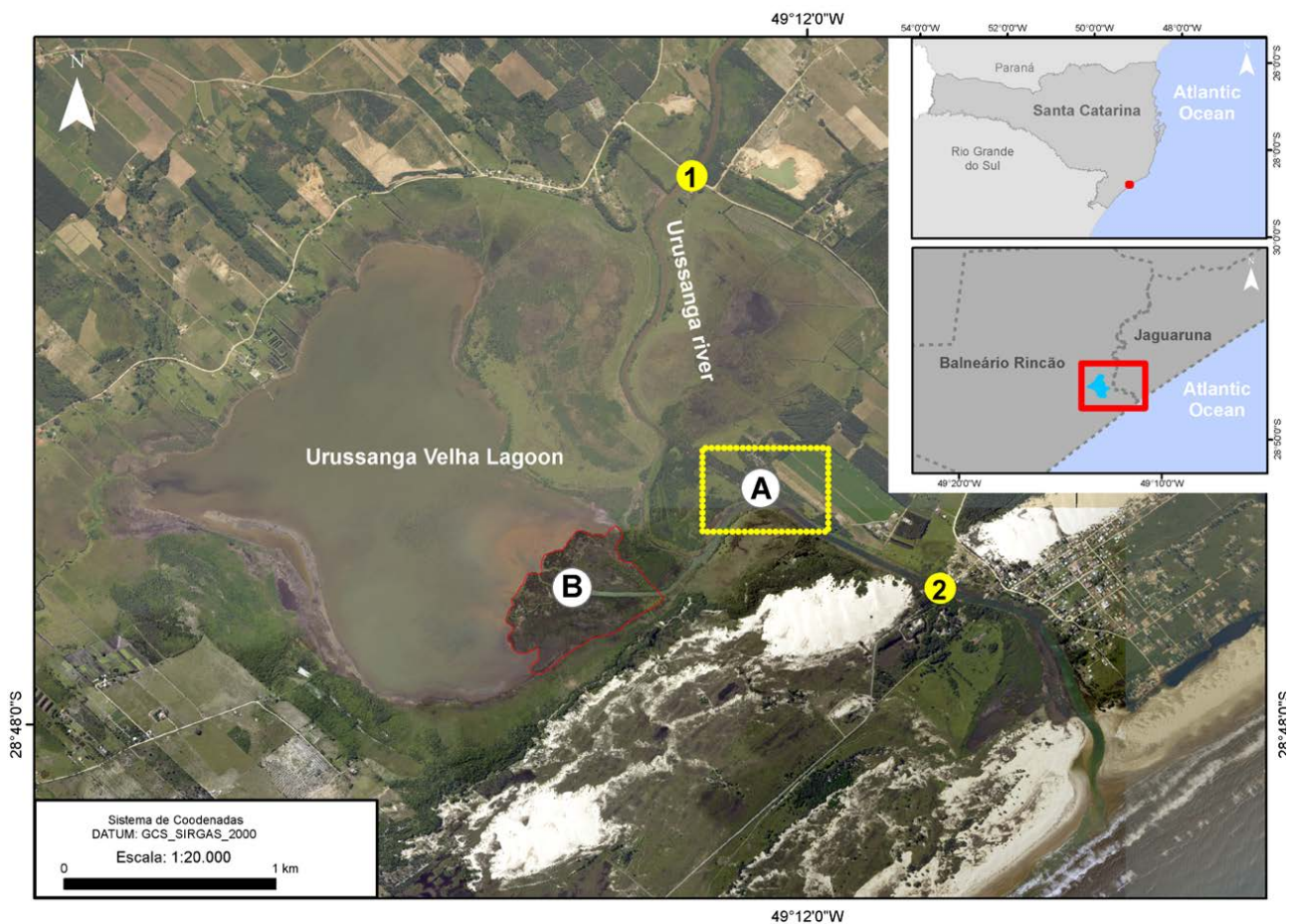


Figure 1. The study area is located in the southern Santa Catarina coastal plain, at the border between the municipalities of Balneário Rincão and Jaguaruna. (1) water sampling station 1; (2) water sampling station 2. (A) insert of the location of Figure 2, emphasizing the confluence of the Urussanga River; (B) Intra-lagoon delta of the Urussanga Velha Lagoon (Data source: Continuous Cartographic Base of Brazil on the millionth scale – BCIM version 4 – 2014, in SIRGAS2000, geographic coordinate system, data from federal, state, and municipal sector agencies. Image source: SDE-SC).

Figura 1. Área de estudo está localizada na planície costeira do sul de Santa Catarina, na divisa dos municípios de Balneário Rincão e Jaguaruna. (1) estação de amostragem de água 1; (2) estação de amostragem de água 2. (A) inserção do local da Figura 2, com destaque para a confluência do rio Urussanga; (B) Delta intralagunar da Lagoa Urussanga Velha (Fonte de dados: Base Cartográfica Contínua do Brasil na escala milionésima – BCIM versão 4 – 2014, no SIRGAS2000, sistema de coordenadas geográficas, dados de órgãos setoriais federais, estaduais e municipais. Fonte da imagem: SDE-SC).

In addition to ENSO, other events have been accounted as responsible for morphological changes in southern Brazil. Recent studies also confirmed the existence of low-frequency climate variability modes, which present decadal to multidecadal scales (Folland *et al.*, 1990; Latif & Bernet, 1994; Zhang *et al.*, 1997; Mantua *et al.*, 1997; Minobe, 1997; Mestas-Nuñez & Enfield, 1999; Leal *et al.*, 2022). These variability modes occur in the Pacific and Atlantic oceans, driving important climatic teleconnections. The Pacific Decadal Oscillation (PDO) is among the main teleconnection configurations affecting global climatic variability that influences South America and southern Brazil (Cavalcanti & Ambrizzi, 2009; Grimm, 2009). Some studies have discussed the relationship between PDO and changes in temperature and rainfall regime in southern Brazil (Streck *et al.*, 2009; Cera *et al.*, 2009; Spinelli & Alves, 2014; Nascimento Jr. & Sant'anna Neto, 2016; Rebello, 2016; Caballero *et al.*, 2018).

2. Material and Methods

2.1 Remote Sensing

The delta's geomorphological aspects were evaluated using historical aerial photographs from 1957 (1:30,000) and 1978 (1:25,000), provided by the Sustainable Economic Development Secretariat of the Government of the State of Santa Catarina (Secretaria de Desenvolvimento Econômico Sustentável do Governo do Estado de Santa Catarina – SDE-SC). Orthophotographs (1:10,000) from 2012 were also used (available at <http://sigsc.sds.sc.gov.br/>). The photointerpretation analysis was conducted in a Geographical Information System (GIS) environment using the software ArcMap™ 10.8. First, aerial photographs were georeferenced using control points from the 2012 orthophotographs. Next, the morphological unit was identified considering the following factors: texture, hue, structures, and characteristic topographic forms.

2.2 Climatic Indices

With the objective of evaluating and correlating meso- and large-scale (teleconnections) climatic variabilities with the delta's formation period and development, climatic indices were calculated using the MATLAB® R2018a (MathWorks) packages Climate Data Toolbox for MATLAB® (Greene *et al.*, 2019) and Get Climate Teleconnection Indices (Greene *et al.*, 2020). Time series data of the indices used were obtained from the National Oceanic and Atmospheric Administration (NOAA) (www.ncdc.noaa.gov/teleconnections/).

The Pacific Decadal Oscillation Index (PDOI) was calculated using monthly values for the period between 1854 and 2020 with moving average (MA) of values with an interval of 120 months, so to smoothen the graph and better evaluate correlations, as indicated by NOAA's guidelines (www.ncdc.noaa.gov/teleconnections/). In addition, the occurrence of El Niño – Southern Oscillation (ENSO) events was evaluated using the Southern Oscillation Index (SOI) for the period between 1878 and 2020 to corroborate the information and investigate the existence of any correlation between the data.

Local and regional climatological data was gathered from the Meteorological Data Bank for Education and Research (Banco de Dados Meteorológicos para Ensino e Pesquisa - BDMEP) of the Brazilian National Institute of Meteorology (INMET) and the historical database of the Santa Catarina Environmental Resources and Hydrometeorology Information Center (Centro de Informações de Recursos Ambientais e de Hidrometeorologia de Santa Catarina - CIRAM) of the Agricultural Research and Rural Extension Agency of Santa Catarina (EPAGRI). Rainfall data was gathered from the

Brazilian National Water and Sanitation Agency's (ANA) HidroWeb website (www.snirh.gov.br/hidroweb/serieshistoricas).

2.3 Hydrodynamics and Water Parameters

The Urussanga River fluvial-estuarine system was divided into three regions to better understand and represent its dynamics: upstream (1), downstream (2), and distributary (3), using the confluence between the distributary channel that migrates to the lagoon and the main river channel as reference (Fig. 2).

To identify hydrodynamic patterns in the Urussanga River estuary, satellite images available from Google Earth® Pro for the area (between 2011 and 2019) were analyzed. During field campaigns, aerial photographs were obtained using a drone. Data acquisition consisted basically of three phases: planning, execution or collection, and data processing/analysis. Image analysis was conducted using remote sensing techniques. The main element used for analysis was hue (color). A correlation between the color patterns found and climatological data (rainfall) was determined.

Water parameters (salinity and turbidity) were measured in two sampling stations along the estuary. Station 1 was located 4 km from the river mouth, while station 2 was approximately 1.5 km away (see Fig. 1). An AQUAREAD AP-800 multiparameter probe was used to measure these parameters.

During the field campaign in 2019, a MAVIC 2 PRO (DJI®) drone was used, operated through the DJI GO4 application (free flight), to obtain images of the conditions in the suspended material in the water column.

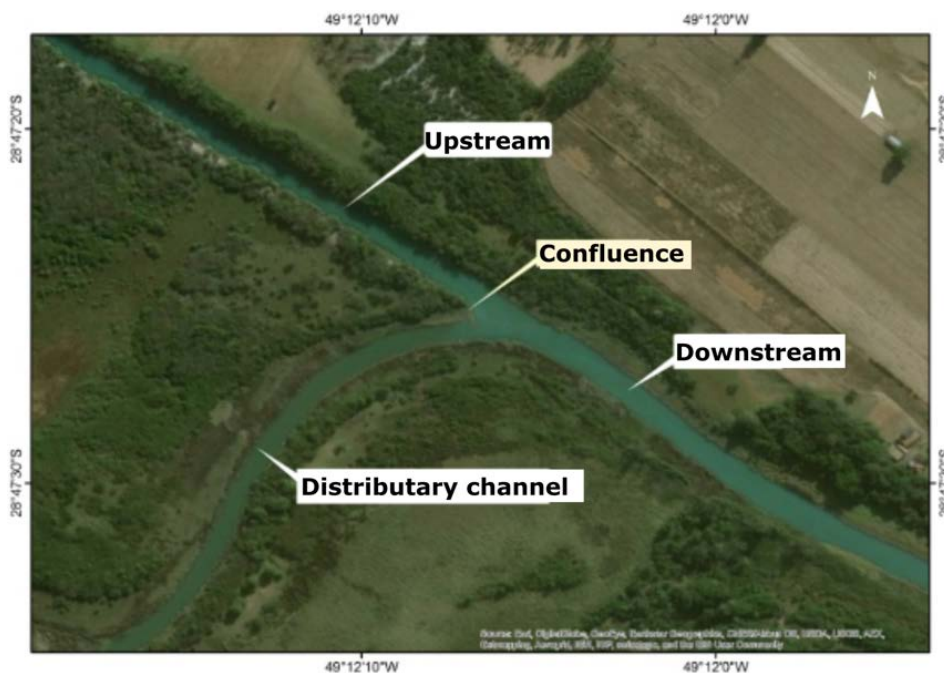


Figure 2. Subdivision of the Urussanga River fluvial-estuarine system. Distributary channel that connects the system with the Urussanga Velha Lagoon. The location is indicated in Figure 1. (Image source: Basemap ArcMap™ 10.8).

Figura 2. Subdivisão do sistema flúvio-estuarino do rio Urussanga. Canal afluente que liga o sistema à Lagoa Urussanga Velha. A localização é indicada na Figura 1. (Fonte da imagem: Basemap ArcMap™ 10.8).

Rainfall data was obtained from BDMEP, and recorded by conventional meteorological stations of INMET's network of stations. The station used for data retrieval was URUSSANGA (OMM 83923), located within the Urussanga River watershed, approximately 35 km away from the study area.

Sea level data were recorded by EPAGRI/CIRAM's telemetric stations (automated) (EPAGRI, 2020). Harmonic constants for the predicted astronomical tide level were calculated using a year-long dataset gathered through the Imbituba tide gauge. The sea level observed is made available every hour through the tide gauge of the Balneario Rincão station, located 3.5 km southwards from the mouth of the Urussanga River fluvial-estuarine system.

3. Results

3.1 Geomorphological evolution

The spatiotemporal evolution of the intra-lagoon delta of the Urussanga Velha Lagoon was identified through the analysis of aerial photographs (Fig. 3 and Table 1). The images indicated that in 1957 the feature had not yet formed and that the lagoon covered an area of 2.39 km². By 1978 it was possible to see the beginning of the delta development, with an area of 0.13 km², while the total area of the lagoon reduced by 12% (2.10 km²). The image from 2012 showed that the delta doubled in size compared with 1978, presenting a total area of 0.25 km², while the lagoon area decreased by 5% during the same period, going from 2.10 to 2.00 km². These values refer to the images analyzed and variations in the lagoon's water level can partly change them.

Table 2. Spatiotemporal evolution relationship of the delta and the Urussanga Velha Lagoon.

Tabela 1. Relação de evolução espaço-temporal do delta e da lagoa Urussanga Velha.

DELTA		LAGOON	
YEAR	AREA (km ²)	YEAR	AREA (km ²)
1957	0	1957	2.39
1978	0.13	1978	2.10
2012	0.25	2012	2.00

An important fact to highlight is that sometime between 1957 and 1978 part of the Urussanga River was straightened (red dashed line, Fig. 3B). This intervention resulted in changes to the dynamics of the fluvial system. An example of such a change was the later abandonment of the river's meander.

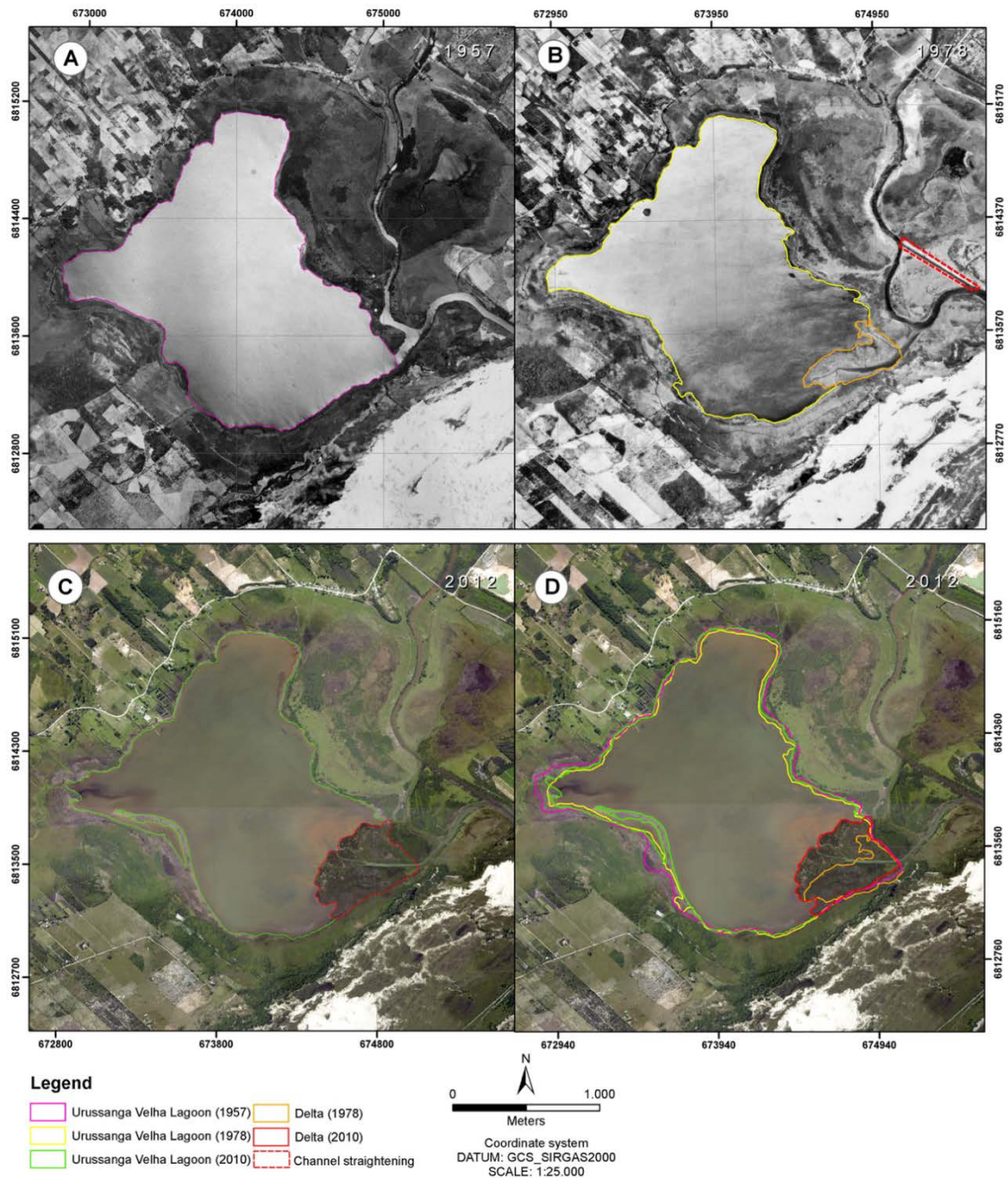


Figure 3. (A) Aerial photograph from 1957. (B) Aerial photograph from 1978. (C) Orthophotograph from 2012. (D) Orthophotograph from 2012 with analysis showing the spatiotemporal evolution of the intra-lagoon delta and the Urussanga Velha Lagoon between 1957 and 2012.

Figura 3. (A) Fotografia aérea de 1957. (B) Fotografia aérea de 1978. (C) Ortofotografia de 2012. (D) Ortofotografia de 2012 com análise mostrando a evolução espaço-temporal do delta intralagunar e da lagoa Urussanga Velha entre 1957 e 2012.

3.2 Climatic Data and Teleconnections

The MATLAB[®] packages used allowed to obtain several teleconnection indices (Greene *et al.*, 2019, 2020). However, PDO was defined as the one that best applied to the present study because its influence on the climatic pattern in southern Brazil has already been discussed by several authors (Sperling *et al.*, 2009; Streck *et al.*, 2009; Cera *et al.*, 2009; Spinelli & Alves, 2014; Nascimento Jr & Sant’anna Neto, 2016; Leal *et al.*, 2021).

The 120-month moving average allowed to identify the presence of four negative periods (cold phase) and three positive ones (warm phase) for PDO (Fig. 4A). The first cold phase began before 1860 and lasted until 1900. The other ones occurred between 1911-1925, 1946-1978, and 1996-2018. Warm phases were identified between 1901-1910, 1926-1945, and 1979-1995. The annual moving average clearly showed a pattern shift that occurred during the late 1970s.

The occurrence of ENSO between 1868 and 2020 was also evaluated (Fig. 4B) to corroborate the information gathered and to investigate the existence of any correlation between the data. Positive values (blue) refer to La Niña periods while negative ones (red), to El Niño periods.

3.3 Image analysis

A total of 23 images available from Google Earth® Pro were analyzed in a Geographic Information System (GIS) - ArcMap™. However, only six of them presented enough quality for photointerpretation (Fig. 5). In images (A), (B), (D), and (F), the color of the water downstream was the same as upstream, while in the distributary channel, it was different. In the image (C), all three regions presented different colors. In the image (E), the colors upstream were the same as in the distributary channel, and the color of the water downstream was different from both. Accumulated rainfall (previous five days) ranged between 1 and 29 mm.

3.4 Hydrodynamic data (seawater level) and Water parameters

During the first field campaign (Figs. 6A and 7A), the difference between the observed level (OL) and the astronomical tide (AT) was 15 cm, above the predicted level. Considering the mean value of the difference between OL and AT 24 hours before the field campaign, a value of 12 cm above the predicted level was observed. Regarding water parameters, salinity at station 1 varied between 1.3 and 1.6, and the highest values were recorded at greater depths (3.2 m). Water turbidity ranged from 5 to 55 NTU, with the highest values found at 2.3 m in depth, and the lowest ones at 3 m in depth. At station 2, salinity varied between 1.2 and 2.4, and the highest values were also found at greater depths. Turbidity ranged from 4 NTU, at the surface layer, to 360 NTU at 4.5 m in depth. At this station, a sharp change in turbidity was observed after reaching 3 m in depth.

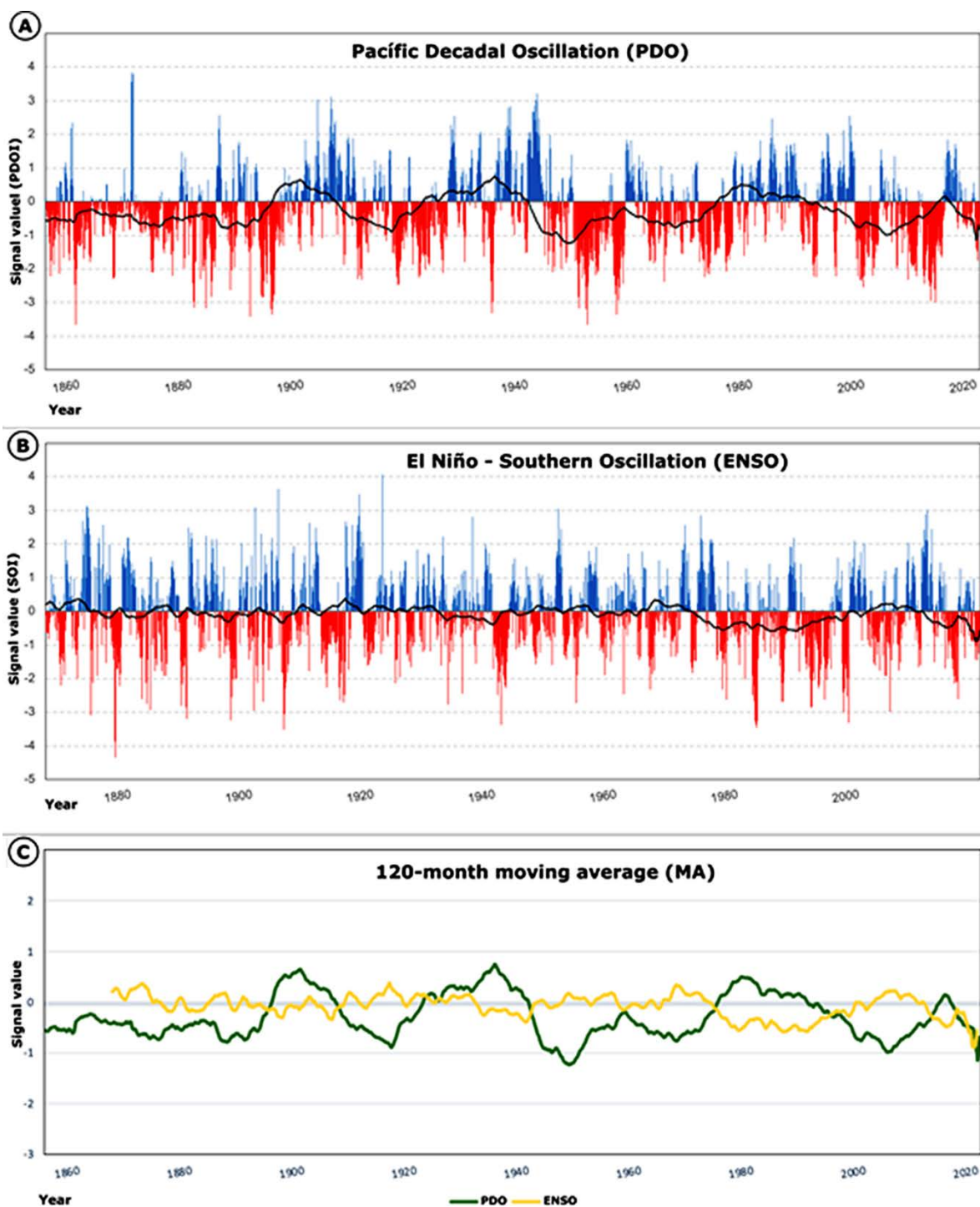


Figure 4. (A) Pacific Decadal Oscillation time series for the period between January 1854 and February 2020. Positive values represent warm phases and negative ones, cold phases. (B) El Niño – Southern Oscillation time series between January 1868 and February 2020. Positive values refer to La Niña periods and negative ones, to El Niño periods. Black lines in (A) and (B) refer to the moving average of values of signals accumulated for 10 years, also represented in (C). The indices' values are available on NOAA's website at www.ncdc.noaa.gov/teleconnections/.

Figura 4. (A) Série temporal da Oscilação Decadal do Pacífico para o período entre janeiro de 1854 e fevereiro de 2020. Valores positivos representam fases quentes e negativos, fases frias. (B) Série temporal El Niño – Oscilação Sul entre janeiro de 1868 e fevereiro de 2020. Os valores positivos referem-se a períodos de La Niña e os negativos, a períodos de El Niño. As linhas pretas em (A) e (B) referem-se à média móvel dos valores dos sinais acumulados por 10 anos, também representados em (C). Os valores dos índices estão disponíveis no site da NOAA em www.ncdc.noaa.gov/teleconnections/.

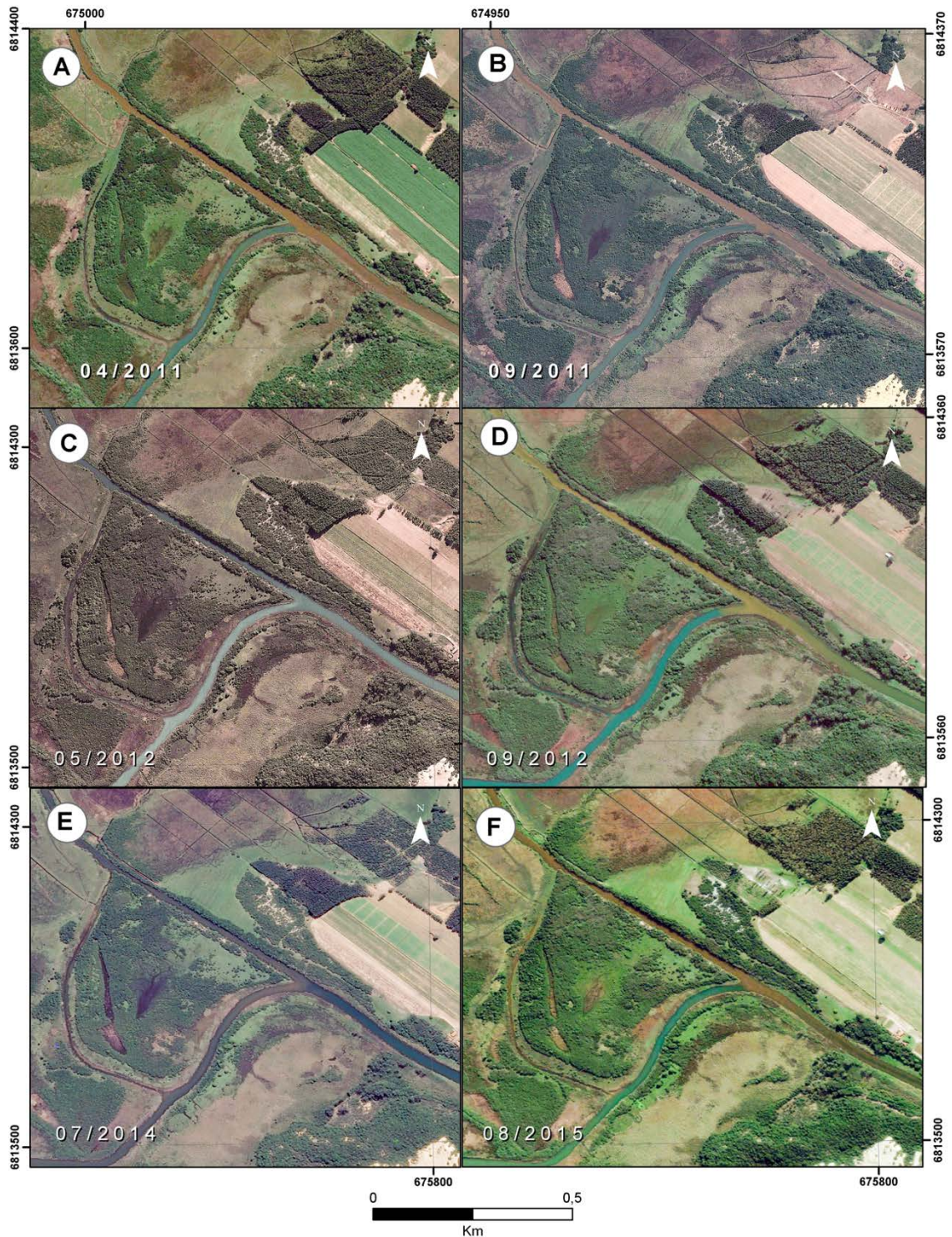


Figure 5. Satellite images from Google Earth® from several dates showing the hydrodynamic behavior of the Urussanga River fluvial-estuarine system based on the color of the water in the upstream, downstream, and distributary channel regions. A and B) 2011 yr; C and D) 2012 yr; E) 2014 yr; and F) 2015 yr.

Figura 5. Imagens de satélite do Google Earth® de várias datas mostrando o comportamento hidrodinâmico do sistema fluvial-estuarino do rio Urussanga com base na cor da água nas regiões de montante, jusante e canal de distribuição. A e B) ano de 2011; C e D) ano de 2012; E) ano de 2014; e F) ano de 2015.

The rainfall accumulated over the five days prior to fieldwork was 77.2 mm. Drone images showed brown water downstream and upstream as a result of high turbidity (suspended sediment), while the distributary channel presented a different pattern, with dark green waters and not much-suspended sediment.

During the second field campaign (Figs. 6B and 7B), the difference between OL and AT was 27 cm, above the predicted level. The mean value of the difference between OL and AT 24 hours before the field campaign yielded a value of 14 cm, above the predicted level. Salinity at station 1 did not vary, maintaining the measurement of 0.05 from surface to bottom (2.6 m). Turbidity ranged from 5 to 18 NTU, with the highest values recorded at 2.3 m in depth, and the lowest ones, at 3 m in depth. At station 2, salinity varied between 2.7 and 27, presenting its lowest values at 1.5 m in depth, and the highest between 3 and 4 m. Water turbidity ranged from 6 NTU near the surface to 54 NTU at 2.7 m in depth. The rainfall accumulated over the five days before sampling was 13.4 mm. Field observations allowed to understand the dynamics of the estuary at the moment when the images were taken, showing that the ebb flow of the river has deviated from the upstream sector to the distributary channel (Fig. 9B).

During the third field campaign (Figs. 6C and 7C), the difference between OL and AT was 17 cm, above the predicted level. Considering the mean value of the difference between OL and AT 24 hours before the campaign, the value observed was 6 cm, above the predicted level. At station 1, salinity did not vary vertically, again remaining at 0.05 from the surface to the bottom layer (2.6 m). Water turbidity ranged from 16 to 24 NTU, with the highest values recorded at 2.5 m in depth and the lowest ones, at 0.5 m. At station 2, salinity varied between 2.4 and 24, presenting the lowest values until 1.5 m in depth, and the highest between 3 and 5 m. Turbidity ranged from 6 NTU, close to the surface, to 45 NTU at 2.7 m in depth. The rainfall accumulated over the five days before the campaign was 17 mm.

During the fourth field campaign (Figs. 6D and 7D), the difference between OL and AT was 5 cm, above the predicted level. Considering the mean value of the difference between OL and AT 24 hours before the campaign, the value observed was 3 cm, above the predicted level. Again, at station 1, the water column was homogeneous, in other words, a constant salinity value (0.05) was recorded from surface to bottom. Water turbidity ranged from 5 to 18 NTU, with the highest values found at 2.3 m in depth and the lowest ones at 3 m. At station 2, salinity varied between 2.4 and 24, presenting the lowest values until 1.5 m in depth, and the highest ones between 3 and 5 m. Turbidity ranged from 5 to 16 NTU, and the lowest values were found at the deepest points in the water column (4.6 m). The rainfall accumulated over the five days before the campaign was 0.2 mm.

4. Discussion

4.1 Evolution, Climatic Data, and Teleconnection

The period required to form the intra-lagoon delta was considered associated with the PDO warm phase that occurred between 1977 and 1998, described by Mantua & Hare (2002). This warm phase, which started during the late 1970s, resulted in an increase in rainfall in southern Brazil, as observed by Martinho *et al.* (2010), Miot da Silva & Hesp (2013), Sant Ana & Back (2019). This resulted in more humid climatic conditions for the region, which influenced the morphology of Holocene barriers in southern Brazil (Miot da Silva & Hesp, 2013; Miot da Silva *et al.*, 2013). These conditions may have favored a higher sediment input to the Urussanga River fluvial-estuarine system and consequently supplied it with material to form the intra-lagoon delta.

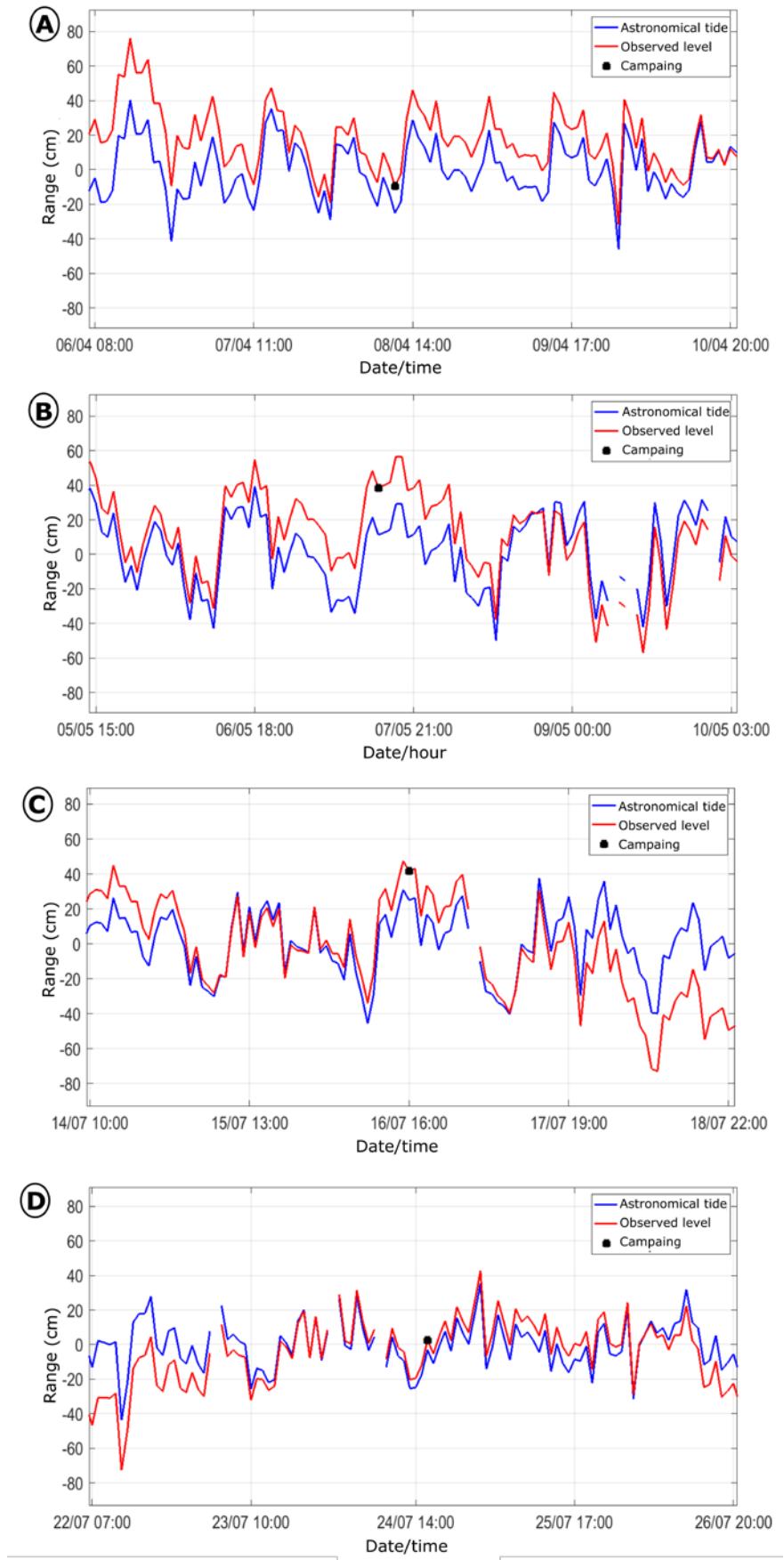
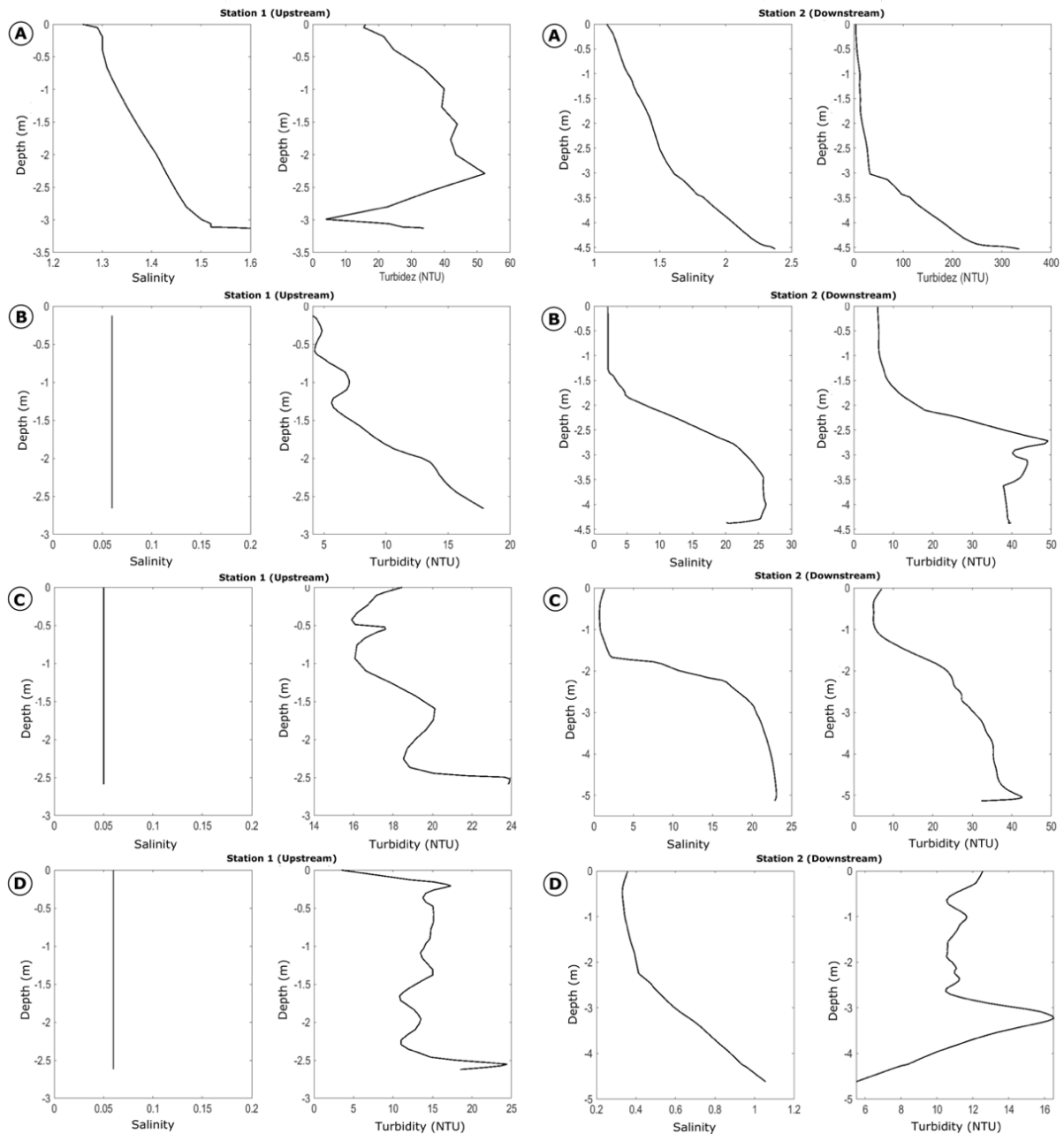


Figure 6. Astronomical tide and observed tide level ranges during field campaigns.

Figura 6. Maré astronômica e intervalos de nível de maré observados durante campanhas de campo.



Accumulated rainfall (mm)	A	B	C	D
	77	13.4	17	0.2

Figure 7. Water parameters (salinity and turbidity) measured during field campaigns. Station 1 (upstream) is located 4 km from the river mouth, and station 2 (downstream) is approximately 1.5 km away (see Fig. 1). Accumulated rainfall refers to the five days prior to campaigns.

Figura 7. Parâmetros da água (salinidade e turbidez) medidos durante as campanhas de campo. A estação 1 (a montante) está localizada a 4 km da foz do rio, e a estação 2 (a jusante) está a aproximadamente 1,5 km de distância (ver Fig. 1). A precipitação acumulada refere-se aos cinco dias anteriores às campanhas.

PDO has been approached in recent scientific literature as an important low to very low-frequency variability mode (Cavalcanti & Oliveira, 1996; Cavalcanti & Ambrizzi, 2009; Kayano & Andreoli, 2006; 2009; Grimm, 2009) and can be described as having similar behavior to ENSO, though with different time configurations (Mantua & Hare, 2002). The repercussions of PDO last longer and are therefore more stable and better able to correlate with geomorphological indicators (Nigam & Baxter, 2015).

From the mid-1970s onwards, a pattern change was observed regarding ENSO behavior, when El Niño events predominated. This phenomenon is known to cause periods of high rainfall levels in southern Brazil (Diaz *et al.*, 1998; Grimm *et al.*, 1998). Before 1975, La Niña predominated, an event associated with atmospheric blockages and consequently below-average rainfall levels. According to studies by Gershunov & Barnett (1998), Mantua *et al.* (1997), and Zhang *et al.* (1997), PDO and ENSO can determine combined implications in the anomalous rainfall distribution of some regions, acting “constructively” with strong, well-defined anomalies when they are in the same phase, and “destructively” with weak, poorly-defined anomalies when they are in opposite phases.

The comparison between PDOI and SOI allowed to observe that during the PDO positive phase, ENSO was in its negative phase, when there was a higher occurrence of El Niño. On the other hand, during the PDO negative phase, between 1946 and 1978, a higher number of La Niña events occurred. This inverse behavior of climatic modes has already been discussed by other authors, such as Mantua *et al.* (1997), and Kayano & Andreoli (2006; 2009). Between 1978 and 1999, events clearly acted “constructively” with strong, well-defined anomalies (PDO warm phase + El Niño) (see Fig. 4C).

In addition to influencing rainfall patterns, ENSO is widely known for influencing sea level in the Pacific Ocean in low frequencies (for example, Clarke & Van Gorder, 1994; Nerem *et al.*, 1999; Li & Clarke, 2007). In southern Brazil, winds that blow from the southern quadrant result in water transport from the open sea towards the coast (Ekman Transport), causing an accumulation of water on the coast and, consequently, an increase in low-frequency sea-level rise, in an effect known as storm surge (Truccolo *et al.*, 2006). Winds from this quadrant are caused by the passing of frontal systems, which are associated with extratropical cyclones (Calliari *et al.*, 1998; Parise *et al.*, 2009). According to Pereira *et al.* (2012), although La Niña is responsible for the high occurrence of extratropical cyclones in southern Brazil, cyclones are more dominant during El Niño as changing factors for the region’s climate, especially by increasing the intensity of southerly winds, and consequently increasing low-frequency sea-level rise. Still, according to the authors, this behavior occurs because during La Niña periods extratropical cyclones are more ephemeral and occur in a region far from the coast, not expressively influencing low-frequency sea level. In turn, during El Niño, cyclones occur closer to the coast and last longer, leading to a higher incidence of southerly winds over more hours during El Niño, causing greater influence on low-frequency sea levels. Pereira *et al.* (2012) reported that months that corresponded to El Niño had a much higher influence on the hydrodynamics of the Patos Lagoon estuary (RS) than La Niña months, for example.

4.2 Remote Sensing and Hydrodynamics

Based on the location (upstream, downstream, and distributary channel) of “water masses” with different colors, two hydrodynamic patterns were identified in the Urussanga River fluvial-estuarine system: (1) continent-ocean flow, and (2) continent-lagoon flow (Fig. 8).

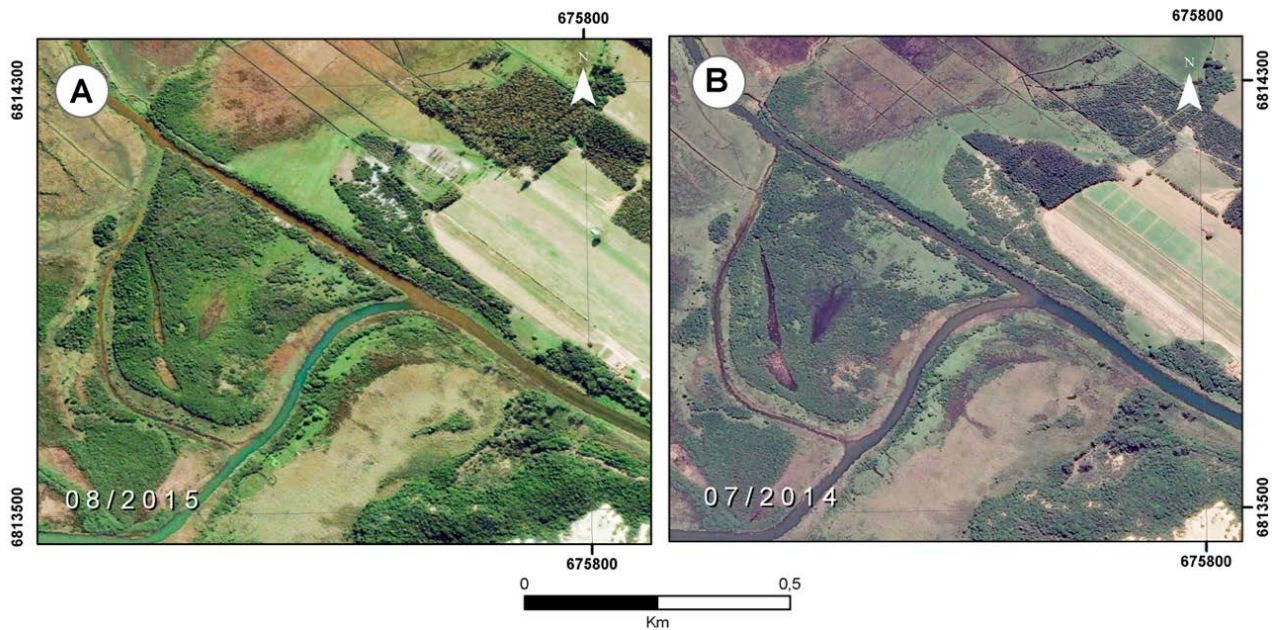


Figure 8. Hydrodynamic patterns identified in the Urussanga River fluvial-estuarine system using photointerpretation of satellite images obtained from Google Earth® Pro.

Figura 8. Padrões hidrodinâmicos identificados no sistema fluvial-estuarino do rio Urussanga por meio de fotointerpretação de imagens de satélite obtidas do Google Earth® Pro.

In pattern 1 (Fig. 8A), the color of the water both upstream and downstream of the channel was the same. Of the images analyzed, four presented this pattern (See Fig. 4A, 4B, 4E, 4F). This was observed during the first field campaign when the high accumulated rainfall (77.2 mm) was the main driver of estuarine hydrodynamics (Fig. 9A). This behavior was observable because of the high turbidity level upstream and downstream from the estuary, and due to the low salinity downstream. However, regardless of the high rainfall recorded, station 1, located approximately 4 km away from the river mouth, presented salinity at its bottom layer. This resulted from storm surge influence in the estuary, which during the campaign period and previous days, was approximately 0.40 cm above the mean level (see Figs. 6A and 7A).

In pattern 2 (Fig. 8B), the river flow was deviated to the lagoon. This was corroborated by the similarity in the color of the water between the distributary channel and the upstream region. In the field, during the second and third campaigns, a hydrodynamic flow in which the flood flow (opposed to the river-ebb flow) caused the deviation of the river flow to the distributary channel, and therefore into the lagoon (Figs. 9B and 9C). This pattern occurred when storm surge levels reached approximately 0.40 cm in campaigns 1 and 2, and the accumulated rainfall was 13.4 and 17 mm, respectively. In other words, even with relatively high rainfall values, the influence of low-frequency positive sea-level changes tended to cause pattern 2.

As Dyer (1995) and Uncles *et al.* (2002) affirmed, estuarine sedimentary dynamics vary significantly in each estuary, over time, and in space within a single estuary due to the various factors involved, making it complex to conduct studies on sedimentary transport in this environment.



Figure 9. Aerial photographs obtained using a drone during the campaign days (2019) showing the hydrodynamics of the Urussanga River fluvial-estuarine system in various climatological and oceanographic conditions. A) Normal condition with flow from the river to the sea; B) Meteorological tide condition; and C) Meteorological tide condition and flow associated with winter precipitation.

Figura 9. Fotografias aéreas obtidas com drone durante os dias de campanha (2019) mostrando a hidrodinâmica do sistema fluvial-estuarino do rio Urussanga em diversas condições climatológicas e oceanográficas. A) Condição normal com fluxo do rio para o mar; B) Condição de maré meteorológica; e C) Condição de maré meteorológica e fluxo associado às precipitações de inverno.

5. Conclusion

Important climatological variations, with repercussions to the region studied, began to occur in the 1970s. This period was characterized by the end of the PDO cold phase (beginning in 1946) and the beginning of a warm phase, and by the beginning of a period dominated by positive ENSO events (El Niño). Both climatic variability modes are associated with a high occurrence of rainfall in the region, which consequently provided a high availability of sediments in the Urussanga River fluvial-estuarine system. In addition to influencing the increase in rainfall, periods, when El Niño predominated, tend to result in a high occurrence of positive storm surges, which, as discussed by other authors, influence the hydrodynamics of coastal environments, such as estuaries and coastal lagoons.

The river flow naturally tends to follow pattern 1 due to its natural dynamics associated with morphological characteristics. When the rainfall factor is added to the system, meaning when a high fluvial discharge is present, this pattern is even more favored. However, rainfall is not the only factor that controls the dynamics of the estuary, given that rainfall also occurred in other scenarios where the estuarine system pattern was different (pattern 2). This other pattern is influenced by sea level, especially by the meteorological component, because the pressure gradient acts as a “hydraulic barrier”, deviating the flow of the main channel into its tributary. This process is responsible for sediment transport to the lagoon and, consequently, for forming the delta.

Since before 1957, the river presented a natural connection with the ocean and with the lagoon. However, there was no indication of the presence of the delta. The straightening of the river channel (sometime between 1957 and 1978) may also have contributed to or intensified the formation of the delta.

Acknowledgments: The authors thank the Conselho Nacional de Desenvolvimento Científico e Tecnológico (CNPq) for the provision of their research fellowships.

CRedit authorship contribution statement: Conceptualization, R.A.L., E.G.B., and M.M.A.; methods, R.A.L., M.M.A. and V.J.B.B.; software, R.A.L., M.M.A., and V.J.B.B.; data preparation, R.A.L., M.M.A., and V.J.B.B.; writing, R.A.L., E.G.B., and M.M.A.; revision, R.A.L., E.G.B. M.M.A., and V.J.B.B.; The authors have read and agree with the published version of the manuscript.

Declaration of competing interest: The authors declare that they have no known competing financial interests or personal relationships that could have appeared to influence the work reported in this paper.

References

- Alvares, C.A., Stape, J.L., Sentelhas, P.C., Gonçalves, J.L.M. and Sparovek, G., 2014. Köppen's climate classification map for Brazil. *Meteorologische Zeitschrift*, 22: 711-728. <https://doi.org/10.1127/0941-2948/2013/0507>
- Andrade, M.M., Toldo, E.E. & Nunes, J.C. 2018. Tidal and subtidal oscillations in a shallow water system in southern Brazil. *Brazilian Journal of Oceanography*, 66: 245-254. <https://doi.org/10.1590/S1679-87592018017406603>
- Angulo, R.J., Souza, M.C., Giannini, P.C.F., Dillenburg, S.R., Barboza, E.G., Rosa, M.L.C.C., Hesp, P.A. & Pessenda, L.C.R. 2022. Late-Holocene sea levels from vermetids and barnacles at Ponta do Papagaio, 27° 50' S latitude and a comparison with other sectors of southern Brazil. *Quaternary Science Reviews*, 286: 107536. <https://doi.org/10.1016/j.quascirev.2022.107536>
- Anthony, E.J. 2014. Deltas. In: Masselink, G., Gehrels, R. (Eds.), *Coastal Environments and Global Change*. John Wiley & Sons Ltd., pp. 299-337.

- Barboza, E.G. & Tomazelli, L.J., 2003. Erosional features of the eastern margin of the Patos Lagoon, southern Brazil: significance for Holocene history. *Journal of Coastal Research*, SI 35: 260-264. <https://www.jstor.org/stable/40928769>
- Barboza, E.G., Rosa, M.L.C.C., Dillenburg, S.R., Biancini da Silva, A. & Tomazelli, L.J., 2014. Stratigraphic analysis applied on the recognition of the interface between marine and fluvial depositional systems. *Journal of Coastal Research*, SI 70: 205-210. <https://doi.org/10.2112/SI70-116.1>
- Barboza, E.G., Dillenburg, S.R., Ritter, M.N., Angulo, R.J., Biancini da Silva, A., Rosa M.L.C.C., Caron, F. & Souza, M.C. 2021. Holocene Sea-Level Changes in Southern Brazil Based on High-Resolution Radar Stratigraphy. *Geosciences (Switzerland)*, 11(8): 326. <https://doi.org/10.3390/geosciences11080326>.
- Becker, C., Barboza, E.G., Martins, E.M. 2021. Uma visão política-administrativa e morfológica dos Balneários Esplanada e Campo Bom do Município de Jaguaruna, SC. *Revista Brasileira de Geomorfologia*, 22 (4): 1-12. <https://doi.org/10.20502/rbg.v22i4.1806>
- Beerbower, I.R. 1966. Cyclothems and cyclic depositional mechanics in alluvial plan sedimentation. *Bulletin - Kansas, State Geological Survey*, 1: 31-42.
- Biancini da Silva, A., Barboza, E.G., Rosa, M.L.C.C. & Dillenburg, S.R., 2014. Meandering fluvial system influencing the evolution of a Holocene regressive barrier in Southern Brazil. *Journal of Coastal Research*, SI 70, 687-692. <https://doi.org/10.2112/SI70-035.1>
- Brusius, B.K., de Souza R.B. & Barbieri E. 2020. Stranding of Marine Animals: Effects of Environmental Variables. In: Leal Filho, W., Azul, A., Brandli, L., Lange Salvia, A., Wall, T. (Eds.), *Life Below Water*. Encyclopedia of the UN Sustainable Development Goals. Springer, Cham. https://doi.org/10.1007/978-3-319-71064-8_102-1
- Caballero, C.B., Ogassawara, J.F., Dorneles, V.R. & Nunes, A.B. 2018. A precipitação pluviométrica em Pelotas/RS: tendência, sistemas sinóticos associados e influência da ODP. *Revista Brasileira de Geografia Física*, 11(4): 1429-1441. <https://doi.org/10.26848/rbgf.v11.4>
- Calliari, L.J., Speranski N.S. & Boukareva, I.I. 1998. Stable focus of wave rays as a reason of local erosion at the Southern Brazilian coast. *Journal of Coastal Research*, 26(2): 19-23.
- Cavalcanti, I.F. & Ambrizze, A.T. 2009. Teleconexões e suas influências no Brasil. In: Cavalcanti, I.F.A., Ferreira, N.J., Silva, M.G.A.J., Dias, M.A.F.S (Eds.), *Tempo e clima no Brasil*. Oficina de Textos, pp. 318-335.
- Cavalcanti, I.F. & Oliveira, G.S. 1996. *Teleconexões*. Climanálise. Centro de Previsão e Tempo e Estudos Climáticos (CPTEC/INPE). Ed. especial. Comemoração de 10 anos.
- Cera, J.C., Teleginski, S.E. & Bender, F.D. 2009. Influência da Oscilação Decadal do Pacífico e as Mudanças no Regime de Chuva do Rio Grande do Sul. *Ciência e Natura*, 31: 317-320. <https://doi.org/10.5902/2179460X9581>
- Clarke, A.J. & Van Gorder, S. 1994: On ENSO coastal currents and sea levels. *Journal of Physical Oceanography*, 24(3): 661-680. [https://doi.org/10.1175/1520-0485\(1994\)024<0661:OECCAS>2.0.CO;2](https://doi.org/10.1175/1520-0485(1994)024<0661:OECCAS>2.0.CO;2)
- Coleman, J.M. & Wright, L.D. 1975. Modern River Deltas: Variability of Processes and Sand Bodies. In: Broussard, M.L. (Ed.), *Deltas: Models for Exploration*. 1a Ed. Houston: Geological Society, pp. 99-149.
- Cowell, P.J., Thom, B.G., Jones, R.A., Everts, C.H. & Simanovic, D. 2006. Management of uncertainty in predicting climate-change impacts on beaches. *Journal of Coastal Research*, 22: 232-245. <https://doi.org/10.2112/05A-0018.1>.
- Dalrymple, R.W. 1999. Tide-dominated deltas: do they exist or are they all estuaries. *American Association of Petroleum Geologists Annual Meeting, Official Program*, p. A29-A30.
- Davis Jr., R.A. & Fitzgerald, D.M. 2004. *Beaches and Coasts*. Blackwell Publishing. UK. 419p.
- Diaz, A.F., Studzinski, C.D. & Mechoso, C.R. 1998. Relationships between precipitation anomalies in Uruguay and southern Brazil and sea surface temperature in the Pacific and Atlantic Oceans. *Journal of Climate*, 11: 251-271. [https://doi.org/10.1175/1520-0442\(1998\)011<0251:RBPUIU>2.0.CO;2](https://doi.org/10.1175/1520-0442(1998)011<0251:RBPUIU>2.0.CO;2)
- Dyer, K.R. 1995. Sediment transport processes in estuaries. In Perillo, G.M.E. (Ed.), *Geomorphology and sedimentology of estuaries*. Developments in Sedimentology, 53. Elsevier Science, pp. 423-449. [https://doi.org/10.1016/S0070-4571\(05\)80034-2](https://doi.org/10.1016/S0070-4571(05)80034-2)

- EPAGRI, 2020. Empresa de Pesquisa Agropecuária e Extensão Rural de Santa Catarina. *Banco de dados de variáveis ambientais de Santa Catarina*. Florianópolis: Epagri. 20p. (Documents, 310).
- Evans, G. 2012. Deltas: the fertile dustbins of the world. *Proceedings of the Geologists' Association*, 123: 397-418. <https://doi.org/10.1016/j.pgeola.2011.11.001>
- Fernandez, G.B., Rocha, T.B., Barboza, E.G., Dillenburg, S.R., Rosa, M.L.C.C., Angulo, R.J., Souza, M.C., Oliveira, L.H.S. & Dominguez, J.M.L. 2019. Natural Landscapes Along Brazilian Coastline. In: Salgado, A.A.R., Santos, L.J.C., Paisani, J.C. (Eds.), *The Physical Geography of Brazil - Environment, Vegetation and Landscape*, pp. 199-218. https://doi.org/10.1007/978-3-030-04333-9_10
- Folland, C.K., Karl, T.R. & Vinnikov, K.Y.A. 1990. Observed climate variations and change. In: *Climate Change: The IPCC Scientific Assessment*, Capítulo 7, pp.195-238.
- Galloway, W.E. 1975. Process framework for describing the morphologic and stratigraphic evolution of deltaic depositional systems. In Broussard, M.L. (Ed.), *Deltas: Models for Exploration*. 1st Ed. Texas: Houston Geological Society, pp. 87-98.
- Gershunov, A. & Barnett, T.P. 1998. Interdecadal modulation of ENSO teleconnections. *Bulletin of the American Meteorological Society*, 79(12): 2715-2726. [https://doi.org/10.1175/1520-0477\(1998\)079<2715:IMOET>2.0.CO;2](https://doi.org/10.1175/1520-0477(1998)079<2715:IMOET>2.0.CO;2)
- Greene, C.A., 2020. *Get Climate Teleconnection Indices*. (<https://www.mathworks.com/matlabcentral/fileexchange/38596-get-climate-teleconnection-indices>), MATLAB Central File Exchange. Retrieved May 4, 2020.
- Greene, C.A., Thirumalai, K., Kearney, K.A., Delgado, J.M., Schwanghart, W., Wolfenbarger, N.S., Thyng, K.M., Gwyther, D.E., Gardner, A.S. & Blankenship, D.D. 2019. *The Climate Data Toolbox for MATLAB*. Geochemistry, Geophysics, Geosystems 2019. <https://doi.org/10.1029/2019GC008392>
- Grimm, A.M., Ferraz, S.E.T. & Gomes, J. 1998. Precipitation anomalies in southern Brazil associated with El Niño and La Niña Events. *Journal of Climate*, 11(11): 2863-2880. [https://doi.org/10.1175/1520-0442\(1998\)011<2863:PAISBA>2.0.CO;2](https://doi.org/10.1175/1520-0442(1998)011<2863:PAISBA>2.0.CO;2)
- Grimm, A.M. 2009. Clima da Região Sul do Brasil. In Cavalcanti, I.F., Ferreira, N.J., Justi Da Silva, M.G.A., Silva Dias, M.A.F.A. (Org.), *Tempo e Clima no Brasil*. Oficina de Textos, São Paulo, pp. 259-276.
- Jerolmack, D.J. & Paola, C. 2010. Shredding of environmental signals by sediment transport. *Geophysical Research Letters*, 37(19): L19401. <https://doi.org/10.1029/2010GL044638>
- Karamitopoulos, P., Weltje, G.J. & Dalman, R.A.F. 2014. Allogenic controls on autogenic variability in fluvio-deltaic systems: inferences from analysis of synthetic stratigraphy. *Basin Research*, 26(6): 767-779. <https://doi.org/10.1111/bre.12065>.
- Kayano, M.T. & Andreoli, R.V. 2006. Relations of South American summer rainfall interannual variations with the Pacific Decadal Oscillation. *International Journal of Climatology*, 27(4): 531-540. <https://doi.org/10.1002/joc.1417>
- Kayano, M.T. & Andreoli, R.V. 2009. Variabilidade decenal a multidecenal. In: Cavalcanti, I.F.A., Ferreira, N.J., Silva, M.G.A.J., Silva Dias, M.A.F. (Org.), *Tempo e Clima no Brasil*. São Paulo: Oficina de Textos, pp. 375-383.
- Kim, W., Paola, C., Voller, V.R. & Swenson, J.B. 2006. Experimental measurements of the relative importance of controls on shoreline migration. *Journal of Sedimentary Research*, 76(2): 270-283. <https://doi.org/10.2110/jsr.2006.019>
- Kinsela, M.A., Hanslow, D.J., Carvalho, R.C., Linklater, M., Ingleton, T.C., Morris, B.D., Allen, K.M., Sutherland, M.D. & Woodroffe, C.D. 2020. Mapping the Shoreface of Coastal Sediment Compartments to Improve Shoreline Change Forecasts in New South Wales, Australia. *Estuaries and Coasts*, 45: 1143-1169. <https://doi.org/10.1007/s12237-020-00756-7>
- Klein, A.H.F., Short, A.D. & Bonetti, J. 2016. Santa Catarina Beach Systems. In: Short, A.D., Klein, A.H.F. (Org.), *Brazilian Beach Systems*. 1st. Switzerland: Springer International Publishing Switzerland, v. 1, pp. 465-506. https://doi.org/10.1007/978-3-319-30394-9_17
- Latif, M. & Barnett, T.P. 1994. Causes of decadal climate variability over the North Pacific and North America. *Science*, 266: 634-637. <https://doi.org/10.1126/science.266.5185.634>

- Leal, R.A., Barboza, E.G., Bitencourt, V.J.R., Biancini da Silva, A. & Manzolli, R.P. 2016. Geological and stratigraphic characteristics of a Holocene regressive barrier in Southern Brazil: GIS and GPR applied for evolution analysis. *Journal of Coastal Research*, SI 75: 750-754. <https://doi.org/10.2112/SI75-151.1>
- Leal, R.A. & Barboza, E.G. 2017. Caracterização geológica, geomorfológica e evolutiva holocênica do litoral sul de Jaguaruna, SC, Brasil. *Pesquisas em Geociências*, 44(3): 417-430. <https://doi.org/10.22456/1807-9806.83265>
- Leal, R.A., Barboza, E.G. & Bitencourt, V.J.R. 2022. Interdecadal climate variability identified in aeolian deposits in southern Santa Catarina, Brazil. *Journal of South American Earth Sciences*, 113, 103636. <https://doi.org/10.1016/j.jsames.2021.103636>
- Li, J. & Clarke, A.J. 2007. Interannual sea level variations in the South Pacific from 5° to 28°S. *Journal of Physical Oceanography*, 37(12): 2882-2894. <https://doi.org/10.1175/2007JPO3656.1>
- Mantua, N.J. & Hare, S.R. 2002. The Pacific Decadal Oscillation. *Journal of Oceanography*, 58: 35-44. <https://doi.org/10.1023/A:1015820616384>
- Mantua, N.J., Hare, S.R., Zhang, Y., Wallace, J.M. & Francis, R.C. 1997. A Pacific interdecadal climate oscillation with impacts on salmon production. *Bulletin American Meteorological Society*, 78(6): 1069-1079. [https://doi.org/10.1175/1520-0477\(1997\)078<1069:APICOW>2.0.CO;2](https://doi.org/10.1175/1520-0477(1997)078<1069:APICOW>2.0.CO;2)
- Martinho, C.T., Hesp, P.A. & Dillenburg, S.R. 2010. Morphological and temporal variations of transgressive dunefields of the northern and mid-littoral Rio Grande do Sul coast, Southern Brazil. *Geomorphology*, 117(1-2): 14-32. <https://doi.org/10.1016/j.geomorph.2009.11.002>
- Mestas-Núñez, A.M. & Enfield, D.B. 1999. Rotated global modes of non-ENSO sea surface temperature variability. *Journal of Climate*, 12(9): 2734-2746. [https://doi.org/10.1175/1520-0442\(1999\)012<2734:RGMONE>2.0.CO;2](https://doi.org/10.1175/1520-0442(1999)012<2734:RGMONE>2.0.CO;2)
- Minobe, S. 1997. A 50–70 year climatic oscillation over the North Pacific and North America. *Geophysical Research Letter*, 24(6): 683-686. <https://doi.org/10.1029/97GL00504>
- Miot da Silva, G. & Hesp, P.A. 2013. Increasing rainfall, decreasing winds, and historical changes in Santa Catarina dunefields, southern Brazil. *Earth Surface Processes and Landforms*, 38(9): 1036-1045. <https://doi.org/10.1002/esp.3390>
- Miot da Silva, G., Martinho, C.T., Hesp, P.A., Keim, B.D. & Ferligoj, Y. 2013. Changes in dunefield geomorphology and vegetation cover as a response to local and regional climate variations. *Journal of Coastal Research*, SI 65: 1307-1312. <https://doi.org/10.2112/SI65-221.1>
- Nascimento Júnior, L. & Sant'anna Neto, J.L. 2016. Contribuição aos estudos da precipitação no estado do Paraná: a oscilação decadal do Pacífico - ODP. *Raega - O Espaço Geográfico em Análise*, 35: 314-343. <https://doi.org/10.5380/raega.v35i0.42048>
- Nerem, R.S., Chambers, D.P., Leuliette, E. W., Mitchum, G.T. & Giese, B.S. 1999. Variations in global mean sea level associated with the 1997- 1998 ENSO event: Implications for measuring long term sea level change. *Geophysical Research Letters*, 26(19): 3005-3008. <https://doi.org/10.1029/1999GL002311>
- Nigam, S. & Baxter, S. 2015. General Circulation of the Atmosphere: Teleconnections. In: North, G.R., Pyle, J., Zhang, F. (Org.), *Encyclopedia of Atmospheric Sciences*. Academic Press, Cambridge: pp. 90-109. <https://doi.org/10.1016/B978-0-12-382225-3.00400-X>
- Orton, G. & Reading, H.G. 1993. Variability of deltaic processes in terms of sediment supply, with particular emphasis on grain size. *Sedimentology*, 40: 475-512. <https://doi.org/10.1111/j.1365-3091.1993.tb01347.x>
- Parise, C.K., Calliari, L.J. & Krusche, N. 2009. Extreme storm surges in the south of Brazil: Atmospheric conditions and shore erosion. *Braz. Brazilian Journal of Oceanography*, 53(3): 75-188.
- Pereira, P.S., Calliari, L.J., Guedes, R.M.C. & Schettini, C.A.F. 2012. Variabilidade temporal da posição dos bancos arenosos da praia do Cassino (RS): uma análise através de imagens de vídeo. *Pesquisas em Geociências*, 39(3): 195-211. <https://doi.org/10.22456/1807-9806.37370>
- Rebello, E.R.G. 2006. As Oscilações Decadais do Pacífico e suas possíveis influências no estado do Rio Grande do Sul. In: XIV CBMET, 2006, Florianópolis - SC. *Anais do XIV CBMET*.
- Rocha M.X. & Rosa, M.L.C.C. 2021. Variabilidade morfodinâmica de deltas intralagunares dolitoral norte do Rio Grande do Sul. *Revista Brasileira de Geomorfologia*, 22(1): 1838. <https://doi.org/10.20502/rbg.v22i2.1838>

- Rosa, M.L.C.C., Barboza, E.G., Dillenburg, S.R., Tomazelli, L.J. & Ayup-Zouain, R.N. 2011. The Rio Grande do Sul (southern Brazil) shoreline behavior during the Quaternary: a cyclostratigraphic analysis. *Journal of Coastal Research*, SI 64: 686-690. <https://www.jstor.org/stable/26482259>
- Rosa, M.L.C.C.; Hoyal, D.C.; Barboza, E.G.; Fedele, J. and Abreu, V.S., 2016. River-dominated deltas: upscaling autogenic and allogenic processes observed in laboratory experiments to field examples of small deltas in southern Brazil. In: Budd, D.A., Hajek, E.A., Purkis, S.J. (Eds.), *Autogenic Dynamics and Self-Organization in Sedimentary Systems*. SEPM Special Publication 106, pp. 176-197. <https://doi.org/10.2110/sepmsp.106.13>
- Rosa, M.L.C.C., Barboza, E.G., Abreu, V.S., Tomazelli, L.J. & Dillenburg, S.R. 2017. High frequency sequences in the Quaternary of Pelotas Basin (coastal plain): a record of degradational stacking as a function of longer-term base-level fall. *Brazilian Journal of Geology*, 47(2): 183-207. <https://doi.org/10.1590/2317-4889201720160138>
- Sant Ana, W.O. & BACK, Á.J. 2019. Tendência do aumento de chuvas e suas implicações na estabilidade de encostas no Sul de Santa Catarina. *Revista Tecnologia e Ambiente*, 25: 95-109. <https://doi.org/10.18616/ta.v25i0.5408>
- Schneider, C. & Gies, D. 2004. Effects of El Niño–southern oscillation on southernmost South America precipitation at 53°S revealed from NCEP–NCAR reanalyses and weather station data. *International Journal of Climatology*, 24(9): 1057-1076. <https://doi.org/10.1002/joc.1057>
- Schossler, V., Simões, J.C., Aquino, F.E. & Viana, D.R. 2018. Precipitation anomalies in the Brazilian southern coast related to the SAM and ENSO climate variability modes. *Revista Brasileira de Recursos Hídricos*. 23: 1-10. <https://doi.org/10.1590/2318-0331.231820170081>
- Siegle, E. & Asp, N.E. 2007. Wave refraction and longshore transport patterns along the Southern Santa Catarina coast. *Brazilian Journal of Oceanography*, 55(2): 109-120.
- Siegle, E. & Calliari, L.J. 2008. High-energy events and short-term changes in superficial beach sediments. *Brazilian Journal of Oceanography*, 56(2): 149-152. <https://doi.org/10.1590/S1679-87592008000200008>
- Sperling, V., Fernandes, V. & Marques, J.R. 2009. Relação entre a oscilação decadal do pacífico (ODP) e a precipitação de verão no rio grande do sul. In: CONGRESSO DE INICIAÇÃO CIENTÍFICA, 18, ENPOS, 9 E mostra científica, 1 – UFPel. *Anais...* Pelotas-RS.
- Spinelli, K. & Alves, D.B. 2014. Geada. In: Hermann, M.L.P. (org), *Atlas de Desastres Naturais do Estado de Santa Catarina: Período de 1980 a 2010*. 2 ed. Florianópolis: IHGSC, GCN/UFSC. 217 p.
- Straub, K.M. & Esposito, C.R. 2013. Influence of water and sediment supply on the stratigraphic record of alluvial fans and deltas: Process controls on stratigraphic completeness. *Journal of Geophysical Research: Earth Surface*, 118(2): 625-637. <https://doi.org/10.1002/jgrf.20061>
- Straub, K.M., Paola, C., Mohrig, D., Wolnsky, M.A. & George, T. 2009. Compensational stacking of channelized sedimentary deposits. *Journal Sedimentary Research*, 79(9): 673-688. <https://doi.org/10.2110/jsr.2009.070>
- Streck, N.A., Paula, G.M., Oliveira, F.B., Schwantes, A.P. & Menezes, N. L. 2009. Improving node number simulation in soybean. *Pesquisa Agropecuária Brasileira*, 44: 661-668. <http://dx.doi.org/10.1590/S0100-204X2009000700002>
- Taschetto, A.S. 2006. *O Impacto do Oceano Atlântico Sul no Clima Regional*. (Tese Doutorado). Universidade de São Paulo, São Paulo, BSP. Recuperado de <http://www.teses.usp.br/teses/disponiveis/21/21132/tde-09082006-152644/>
- Tomer, A., Muto, T. & Kim, W. 2011. Autogenic Hiatus in Fluviodeltaic Successions: Geometrical Modeling and Physical Experiments. *Journal Sedimentary Research*, 81(3): 207-217. <https://doi.org/10.2110/jsr.2011.19>
- Truccolo, E.C., Franco, D. & Schettini, C.A.F. 2006. The low frequency sea level oscillations in the northern coast of Santa Catarina, Brazil. *Journal of Coastal Research*, 39: 547-552.
- Uncles, R.J., Stephens, J.A. & Smith, R.E. 2002. The dependence of estuarine turbidity on tidal intrusion length, tidal range and residence time. *Continental Shelf Research*, 22(11-13):1835-1856. [https://doi.org/10.1016/S0278-4343\(02\)00041-9](https://doi.org/10.1016/S0278-4343(02)00041-9)
- Van Dijk, M., Postma, G. & Kleinhans, M.G. 2009. Autocyclic behaviour of fan deltas: An analogue experimental study. *Sedimentology*, 56(5): 1569-1589. <https://doi.org/10.1111/j.1365-3091.2008.01047.x>

Villwock, J.A., Tomazelli, L.J., Loss, E.L., Dehnhardt, E.A., Horn, N.O., Bachi, F.A. & Dehnhardt, B.A. 1986. Geology of the Rio Grande do Sul Coastal Province. In Rabassa, J. (Ed.), *Quaternary of South America and Antarctic Peninsula* 4, pp.79-97. <https://doi.org/10.1201/9781003079316-5>

Zhang, Y., Wallace, J.M. & Battisti, D. 1997 ENSO-like interdecadal variability: 1900-93. *Journal of Climate*, 10(5): 1004-1020. [https://doi.org/10.1175/1520-0442\(1997\)010<1004:ELIV>2.0.CO;2](https://doi.org/10.1175/1520-0442(1997)010<1004:ELIV>2.0.CO;2)